Bioactive Materials 8 (2022) 196–209

Contents lists available at ScienceDirect

Bioactive Materials

journal homepage: www.sciencedirect.com/journal/bioactive-materials

Natural polymer-derived photocurable bioadhesive hydrogels for sutureless keratoplasty

Xuan Zhao [1], Saiqun Li [1], Xinyue Du, Weihua Li, Qian Wang, Dalian He, Jin Yuan [*]

State Key Laboratory of Ophthalmology, Zhongshan Ophthalmic Center, Sun Yat-sen University, Guangzhou, 510623, China

ARTICLE INFO

Keywords:
Bioadhesive hydrogels
Photocurable
Cornea repair
Sutureless keratoplasty

ABSTRACT

Keratoplasty is the gold standard treatment for visual impairment caused by corneal damage. The use of suturing as the bonding method is the source of many complications following keratoplasty. Currently available corneal adhesives do not have both adequate adhesive strength and acceptable biocompatibility. Herein, we developed a photocurable bioadhesive hydrogel which was composed of gelatin methacryloyl and oxidized dextran for sutureless keratoplasty. The bioadhesive hydrogel exhibited high light transmittance, resistance to enzymatic degradation and excellent biocompatibility. It also had higher adhesive strength than commercial adhesives (fibrin glue). In a rabbit model of lamellar keratoplasty, donor corneal grafts could be closely bonded to the recipient corneal bed and remained attached for 56 days by using of this in situ photopolymerized bioadhesive hydrogel. The operated cornea maintained transparent and noninflamed. Sutureless keratoplasty using bioadhesive hydrogel allowed rapid graft re-epithelialization, typically within 7 days. *In vivo* confocal microscopic and histological evaluation of the operated cornea did not show any apparent abnormalities in terms of corneal cells and ultrastructure. Thus, this bioadhesive hydrogel is exhibited to be an appealing alternative to sutures for keratoplasty and other corneal surgeries.

1. Introduction

The cornea is the clear layer on the front of the eyeball. This structure must remain transparent for optimal vision. Various infectious, inflammatory, degenerative or traumatic disorders can cause corneal scarring, leading to vision impairment and even blindness. Globally, approximately 4.5 million individuals were estimated to have moderately to severely impaired vision because of altered corneal clarity [1]. Corneal transplantation is the main treatment option for visual rehabilitation in patients with corneal blindness [2]. Corneal transplantation typically involves sutures to bond the donor corneal graft to the recipient corneal bed. However, the use of suturing as a bonding method is not only time-consuming and requires a high level of skill but is also associated with numerous potential complications following keratoplasty, including infectious keratitis, sterile infiltrates, corneal neovascularization and high astigmatism [3]. For example, more than half of postkeratoplasty infections are related to the presence or removal of sutures [4]. In addition, sutures typically need to be removed later, which may cause injury to the corneal tissue. For these reasons, sutureless keratoplasty is in certain ways favored over traditional keratoplasty techniques.

Adhesives are appealing alternatives to sutures. Adhesives as bonding methods have been applied in various types of wound closure, such as those in skin [5], bone [6], vessels and heart [7]. The first application of tissue adhesive in ophthalmology was reported in the 1960s [8]. A spectrum of ocular adhesives ranging from synthetic materials to naturally derived polymers have been developed to date, and some of them have obtained approval for clinical use [4,8–11]. In addition to being nontoxic and biocompatible in patients, an ideal adhesive that can replace sutures in corneal transplantation requires various other characteristics, such as being optically transparent to permit vision and having adequate adhesive strength to hold corneal grafts in place.

Cyanoacrylate and fibrin glue are the two most common tissue adhesives in ophthalmology. Cyanoacrylate and its various types have a high tensile strength, but their use in corneal transplantation is not recommended owing to their toxic nature, rough surface, lack of transparency and flexibility, and heat generation during rapid

Peer review under responsibility of KeAi Communications Co., Ltd.
* Corresponding author.
E-mail address: yuanjincornea@126.com (J. Yuan).
[1] Xuan Zhao and Saiqun Li contributed equally.

https://doi.org/10.1016/j.bioactmat.2021.07.001
Received 11 April 2021; Received in revised form 8 June 2021; Accepted 1 July 2021
Available online 6 July 2021

polymerization [12]. By contrast, the transparency, biocompatibility and biodegradability of fibrin-based adhesives make them appealing choices for application in the cornea [13]. Fibrin adhesives have been used in various ocular surgeries to treat corneal perforations, ocular surface disorders and glaucoma [10,14–16]. The use of fibrin adhesives to anchor donor grafts in lamellar keratoplasty (LK) has been reported and yielded promising results [17,18]. However, low adhesion strength is an unavoidable shortcoming of fibrin adhesives and may limit their application in corneal transplantation [4]. In the previous studies, these materials were selectively favored for use in superficial LK. At least 200 μm of residual corneal stromal tissue is recommended to be left at the recipient bed for fibrin glue-assisted sutureless LK [18], but corneal scarring usually involves the deep corneal layers; thus the diseased tissue cannot be completely removed in superficial LK. Moreover, deep anterior lamellar keratoplasty (DALK) has become more popular than superficial LK because it results in superior vision [19]. Viral transmission is another concern for the use of fibrin adhesives, even though these materials are subjected to viral screening and a variety of virus inactivation and reduction treatments are performed [20,21]. Therefore, new corneal sealants that can provide adequate adhesive strength and are also biocompatible are urgently needed.

In recent years, adhesive hydrogels have proven to be effective in closing a variety of wounds, including those in ophthalmology [22–24]. The reported adhesive hydrogels were designed based on different mechanisms, and most of them achieve adhesion via liquid-to-solid transition [24,25]. According to the network strategy, hydrogels can be divided into single-, double- and multiple network gels [26,27]. Adhesiveness is mainly attributable to the chemical or physical interactions between the active group or structure of the adhesives and the tissue [28]. Single-network hydrogels commonly lack interactions with the organization, resulting in poor adhesion to surrounding tissues [26]. To overcome this drawback, a recent study reported enhanced adhesiveness through an interpenetrating secondary network [7]. The concept of double network hydrogels was first proposed in 2003 and has resulted in rapid development in biomedical research and applications [29]. The mechanical strength of hydrogels can be improved through a secondary network. For example, adhesive hydrogels with double networks and extensive chemical interaction could withstand high blood pressure, indicating their possible applications in the repair of arterial, heart [7] and liver [30] bleeding.

Gelatin methacryloyl (GelMA)-based hydrogels have been used as adhesives for the closure of defects in various tissues [7,25,31–33]. GelMA can adhere to body tissue. The use of GelMA alone has achieved success in several tissue defect types, such as volumetric muscle loss [31] and focal corneal defect [25]. However, because its inherent adhesive capacity is weak, a GelMA sealant with higher adhesion strength is required in the settings of wounds that are under great tension. Various approaches have been applied to increase its adhesion strength. In this regard, mussel-inspired hydrogels consisting of DOPA and polydopamine have attracted increasingly attention recently [32,33]. In spite of improved adhesion strength, the mussel-inspired GelMA hydrogels turn into brown color, which makes them not suitable for corneal applications. Moreover, as mentioned above, another recent study designed a double network GelMA hydrogel for the repair of arterial and heart bleeds [7]. But the need of UV light irradiation and dark yellow appearance are their limitations for corneal applications.

Tissue adhesives may require a specific design to account for different application scenarios. Herein, in pursuit of a satisfactory bioadhesive for keratoplasty, we engineered a GelMA-based adhesive hydrogel and enhanced its adhesiveness by introducing oxidized dextran (ODex) to form a double network under visible light. The adhesive formulations were optimized for both adhesiveness and operability. The key physical and chemical properties of the adhesive hydrogel were characterized. Its adhesion effects, biocompatibility and potential clinical translation were further evaluated and investigated in a New Zealand rabbit model of corneal lamellar transplantation.

2. Material and methods

2.1. Materials

GelMA (EFL-GM-60, 60% graft degree) and lithium phenyl-2,4,6-trimethybenzoylphosphinate (LAP) were purchased from Suzhou Intelligent Manufacturing Research Institute (China). Dextran, $NaIO_4$ and diethylene glycol were purchased from Sigma-Aldrich (USA). Dialysis bags (MWCO 8000-14000) were obtained from Guangzhou Qiyun Biotechnology (China). All cell culture related reagents were purchased from Gibco BRL (USA). Calcein acetoxymethyl (calcein AM) and ethidium homodimer-1 LIVE/DEAD assay kit was obtained from Invitrogen (USA). A CCK-8 assay kit was purchased from Dojindo (Japan). An RNeasy Plus Mini Kit was purchased from Qiagen (Germany). PrimerScript RT Master Mix was obtained from TaKaRa Biotechnology (Japan). SYBR Green Supermix was purchased from Bio-Rad Laboratories (USA). Deionized water was obtained using a water purification system (Millipore S. A. S, France).

2.2. Synthesis of ODex and fabrication of bioadhesive hydrogels

ODex was synthesized according to a reported method [34]. 2 g Dextran was dissolved in water at a concentration of 10% (w/v) and 1.6 g $NaIO_4$ was added to the solution. The mixture was stirred at room temperature for 3 h protected from light. An equimolar amount of diethylene glycol was then added. The reacted solution was dialyzed exhaustively for 3 days against deionized water. ODex powder was obtained by lyophilization. The oxidation degree (OD) of ODex was measured as previously described [35]. Briefly, a certain amount of ODex was dissolved in 25 mL of 0.25 mol/L hydroxylamine hydrochloride solution containing 0.05% methyl orange, and allowed to stand at room temperature for 3 h to ensure completely dissolved. The mixture was then titrated with standard sodium hydroxide solution until reaching the red-to-yellow end point. The oxidation degree of ODex can be calculated according to the following equation: $OD = (V_1–V_0) \times M \times M_W/W \times 100\%$, where V_0 = the volume of sodium hydroxide used for blank test; V_1 = the volume of sodium hydroxide used for determination; M = the molar concentration of sodium hydroxide; M_W = the molecular weight of the glucose unit on the dextran chain; W = the weight (g) of ODex. Results represent the average of five batches of samples.

LAP was dissolved in PBS to give a concentration of 0.25% (w/v) and heated at 55 °C to ensure complete dissolution. GelMA powder was dissolved in LAP solution at concentrations of 5%, 10% and 20% (w/v), respectively. Various amounts of ODex were then added to the GelMA solution with mass ratios of GelMA: ODex of 5: 0 (G5), 10: 0 (G10), 20: 0 (G20), 5: 5 (G5OD5), 10: 5 (G10OD5) and 20: 5 (G20OD5) to form prehydrogels. The prehydrogels were incubated at 37 °C for 10 min to form Schiff's bases and then photocrosslinked with visible light (405 nm, 30 mW/cm^2) for 4 min using a light source (Suzhou Intelligent Manufacturing Research Institute, China).

2.3. Microscopic morphology assays

Lyophilized samples were mounted on aluminum stubs and sputter coated with platinum for 70 s before examination by scanning electron microscopy (SEM, EVO18; Zeiss, Germany).

2.4. Evaluation of optical properties

Rectangular hydrogels (3 cm in length, 1 cm in width, 100 μm thick) were prepared as described above. Before testing, samples were immersed in PBS solution (pH = 7.4) for 1 h to completely absorb water. Light transmission was measured with a UV3802 ultraviolet–visible spectrophotometer (Shanghai UNICO, Shanghai, China) at 37 °C in the range of 400–800 nm.

2.5. Water content characterization

The equilibrated water content of the hydrogels was measured as previously described [36]. The samples were immersed in PBS solution (pH = 7.4) for a specific time period. After the hydrogels were quickly blotted with filter paper to remove the superficial water, the weights of the wet samples (M_t) were measured with electronic scales. The swelling ratio of the samples was calculated according to the following equation: $W_t = (M_t - M_0)/M_0 \times 100\%$, where M_0 is the initial weight before swelling. Every reported value was the average of at least five measurements.

2.6. Enzyme resistance assay

The resistance of samples to collagenase was evaluated as described previously [37]. Samples weighing approximately 200 mg were equilibrated for 1 h in 5 mL of 0.1 M Tris–HCl buffer (pH 7.4) containing 5 mM $CaCl_2$ at 37 °C. Subsequently, collagenase (Sigma-Aldrich, USA) solution was added to give a final concentration of 1 mg/mL. The collagenase solution was replaced every 8 h to maintain the collagenase activity. At various time intervals, the samples were taken from the solution, gently blotted on filter paper, and weighed. All samples were tested in triplicate. The percent residual mass of the sample was calculated according to the following equation: residual mass% = $W_t/W_0 \times 100\%$, where W_0 is the initial weight of the hydrogel and W_t is the weight of the hydrogel at each time point.

2.7. Evaluation of mechanical properties

Rectangular hydrogels (3 cm in length, 1 cm in width, 100 μm thick) were prepared as described above. The mechanical properties of the samples were measured as previously described [38]. Before testing, samples were immersed in PBS solution (pH = 7.4) for 1 h to absorb water completely. After gentle blotting on filter paper, two ends of the samples were attached to two pieces of glass slides using superglue and the glass slides were gripped with jaws. The tensile strength, elastic modulus, and elongation at breaking (elasticity) were determined with a uniaxial load testing instrument (Model #5567; Instron Corporation, Issaquah, WA, USA) at a crosshead speed of 5 mm/min and an initial grip separation of 10 mm. The samples were not stress preconditioned before testing to failure. Every reported value was the average of at least five measurements.

2.8. In vitro adhesion tests

The shear adhesive strength of the samples and fibrin glue (Shanghai RAAS Blood Products, China) was tested according to a reported method [38]. Two pieces of glass (7.6 cm in length, 2.6 cm in width) were coated with 20% (w/v) gelatin solution at 37 °C and air dried. Then, 25 μL of prehydrogels solution or mixed fibrin glue was pipetted and photocrosslinked between the two pieces of glass. The bonded area was 2.6 cm by 1 cm. Shear adhesive strengths were measured using a uniaxial load testing instrument (Model #5567; Instron Corporation, Issaquah, WA, USA) at a crosshead speed of 5 mm/min. The shear adhesive strengths were measured at the detachment points.

An *ex-vivo* burst pressure test modified from previous studies was further performed on porcine eyes [25,39]. Corneoscleral buttons were excised from fresh porcine eyes and mounted on Barron artificial anterior chamber (Katena, Denville, USA). A 4-mm penetrating incision was made at the central cornea using 15-degree ophthalmic knife (Alcon, Fort Worth, TX, USA). 15 μL of prehydrogels was applied to the corneal incision sites, followed by in situ cross-linking for 4 min. Artificial anterior chamber was connected to a manometer (HT-1891, Dongguan Xintai Instrument Co., Ltd., China) and a syringe infusion pump (TJ-3A - Single Channel Syringe Pump, Longer Precision Pump Co., Ltd., China). Saline was continuously pumped into artificial anterior chamber at a rate of 5 mL/h. The maximum pressure measured by the manometer is 285 mmHg. The burst pressure was defined as the highest pressure reached before wound leak. The burst pressure of our adhesive hydrogels was compared to that of fibrin glue.

2.9. In vitro cell studies

2.9.1. Cell cultures

Cytotoxicity studies were conducted using murine L929 fibrosarcoma cells (ATCC) because this cell line is widely used for cytotoxicity testing in the literature. Additionally, rabbit corneal fibroblasts were employed to model the transformation process of corneal stromal cells responding to adhesives. L929 cells were maintained in Dulbecco's modified Eagle's medium (DMEM) supplemented with 10% fetal bovine serum (FBS) and 1% penicillin/streptomycin (complete medium). Rabbit corneal fibroblasts were isolated from fresh New Zealand rabbit corneas as previously described [40] and cultured in DMEM containing 10% FBS and 1% penicillin/streptomycin. All cultures were incubated at 37 °C in a humidified atmosphere of 5% CO_2. Subculture by trypsinization with trypsin/EDTA solution was performed when the cells reached to 80% confluence. Cells at passages 3 to 7 were used for the experiments.

Two-dimensional (2-D) culture: The prehydrogels were prepared as described above and filtered through a by 0.22 μm filter (Merck Millipore, USA). Sterile prehydrogels were then added to tissue culture plates and photocrosslinked in the wells. After three washes with culture medium, L929 cells were seeded on top of the hydrogels. The culture medium was replaced every 2 days.

Three-dimensional (3-D) culture: L929 cells were resuspended in sterile prehydrogels. The cell suspension was then added to a tissue culture plate and photocrosslinked in the well to form cell encapsulation. After three washes with culture medium, new culture medium was added to each well and replaced every 2 days.

2.9.2. Assessment of cytocompatibility

The cell viability was evaluated using a LIVE/DEAD assay kit according to the manufacturer's instructions. Calcein AM (0.5 μL/mL) and ethidium homodimer-1 (2 μL/mL) were diluted in DPBS to form the staining solution, which was added to the well after removing the culture medium. Then, the cells were incubated for 30 min at 37 °C in the dark. Live (green stain) and dead (red stain) cells were imaged using an inverted fluorescence microscope (Observer 7, Zeiss, Germany) on days 1, 3 and 5 of culture.

L929 cells were seeded in 96-well tissue culture plates (BD Biosciences) at 5000 cells/cm^2. The leaching medium was prepared by immersing G20OD5 in complete medium at 37 °C for 48 h. The proliferation of L929 cells was quantitatively determined by the CCK-8 assays. The absorbance was measured at 450 nm with a microplate reader at 1, 3 and 5 days of culture.

2.9.3. Quantitative real-time PCR (qRT-PCR)

The expressions levels of the of myofibroblast-related genes Collagen 1A1 (COL1A1), Collagen 3A1 (COL3A1), Fibronectin A1 (FN1) and Transforming growth factor beta 1 (TGF-β1) were measured by qRT-PCR. Total RNA was extracted from rabbit corneal stromal cells using the RNeasy Plus Mini Kit according to the manufacturer's instructions. cDNA was synthesized with PrimerScript RT Master Mix, and qPCR was performed with SYBR Green Supermix using the LightCycler 480 (LC480) Real-Time PCR system (Roche Diagnostics). Relative gene expression was calculated using the delta-delta Cq method after normalization to the reference gene glyceraldehyde-3-phosphate dehydrogenase (GAPDH). The primers sequences were as follows: COL1A1, forward: 5′-GCAAGAACGGAGATGACGGA-3′, reverse: 5′-TTGGCACCATCCAAACCACT-3′; COL3A1, forward: 5′-CCGAACCGTGCCAAATATGC-3′, reverse: 5′-AACAGTGCGGGGAGTAGTTG-3′; FN1, forward: 5′-TTGGTTCAGACTCGAGGTGG-3′, reverse: 5′-

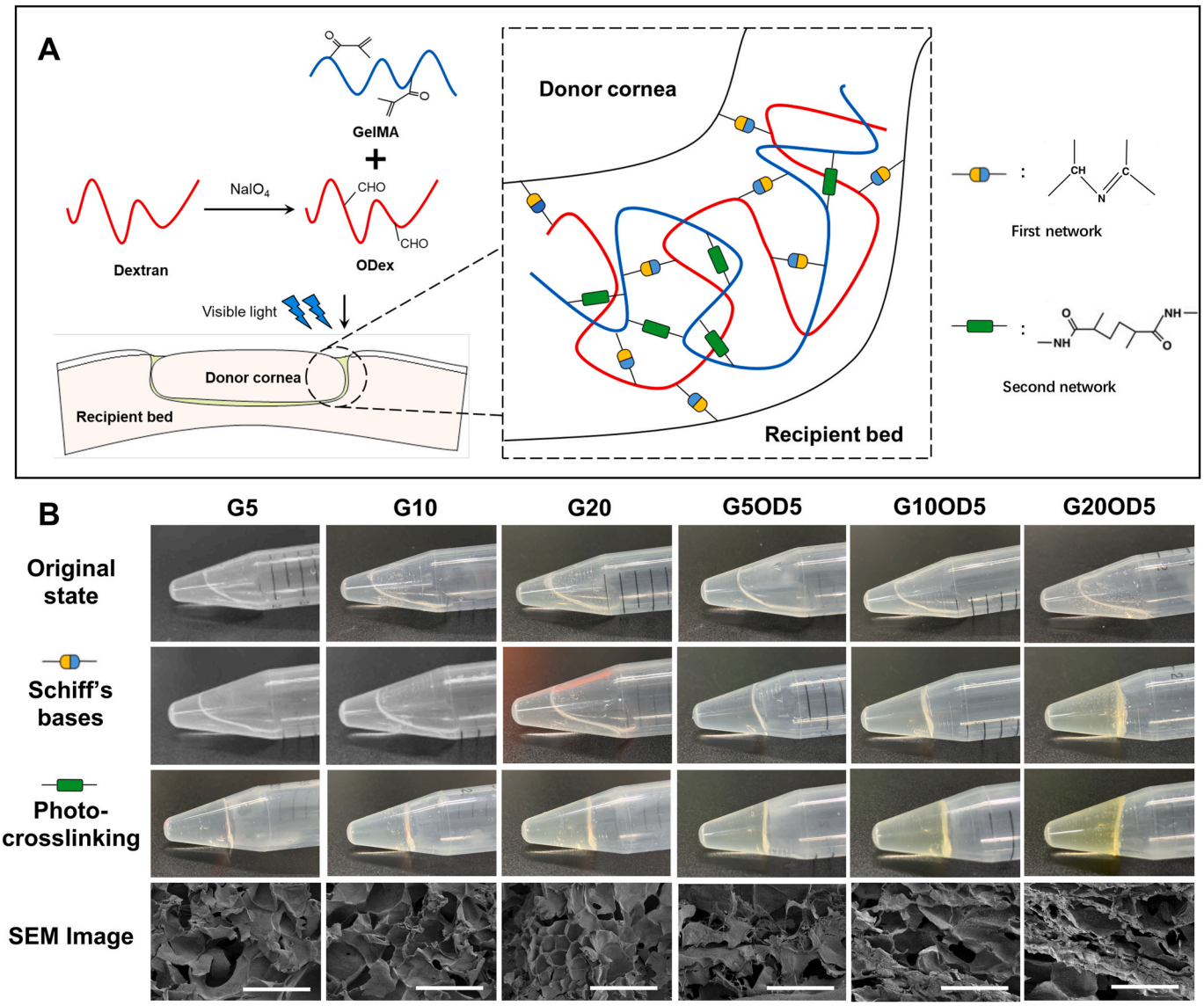

Fig. 1. Fabrication and observation of adhesive hydrogels with different ratios of gelatin methacrylate (GelMA) to oxidized dextran (ODex). (A) Schematic of the synthesis of GelMA-ODex adhesive hydrogel and schematic diagram illustrating its application in sutureless lamellar keratoplasty. (B) Gross comparison of hydrogel formation and scanning electron microscopy (SEM) images of hydrogels with different ratios of GelMA to ODex. Scale bar: 100 μm.

AGATTTCTTCATGGGCAGCCA-3′; TGF-β1, forward: 5′-CTCTGGAACGGGCTCAACAT-3′, reverse: 5′-CTCTGTGGAGCTGAAG-CAGT-3′; GAPDH, forward: 5′-AGGTCGGAGTGAACGGATTTG-3′, reverse: 5′-GCCGTGGGTGGAATCATACT-3′.

2.10. Animal studies

2.10.1. Surgical procedures

All experiments were conducted in compliance with the ARVO statement for the Use of Animals in Ophthalmology and Vision Research and approved by the Animal Care Committees of Zhongshan Ophthalmic Center, Sun Yat-Sen University. 8- to 12-week-old male New Zealand White rabbits (Guangzhou Huadu Hua Dong Xin Hua Experimental Animal Farm, China) were enrolled in this study. LK was performed under general anesthesia with intravenous injection of 2% pentobarbital sodium (30 mg/kg) and topical anesthesia using 0.5% proparacaine hydrochloride ophthalmic solution (Alcon Laboratories). A 6.75 mm trephine was employed to perform partial-thickness trephination in the central host cornea. The anterior corneal stroma was then removed via layer-by-layer manual dissection up to a depth of approximately 2/3. The recipient stroma bed was irrigated with saline to remove any foreign particles and the excessive fluid on the corneal surface was then wiped dry with a sponge. A 0.25-mm oversized donor lenticule with compatible thickness was prepared from the donor rabbit cornea. Approximately 25 μL of temporarily prepared prehydrogels was applied to the recipient stroma bed, and spread out as a thin film with forceps. The donor lenticule was immediately transferred onto the recipient bed and adjusted to the proper position. The two layers were pressed together, and the extra adhesives were squeezed out from the interface. The adhesives were then photopolymerized under 405 nm visible light for 4 min. The extra adhesives at the transplant edge were carefully removed with a sponge. Finally, an Elizabeth collar was used to prevent the animals from scratching their eyes. The postoperative regime included 0.3% tobramycin ointment (Alcon Laboratories) once daily for a week.

2.10.2. Slit-lamp, anterior segment optical coherence tomography (AS-OCT) and confocal microscopy evaluation

Slit lamp biomicroscopy (Topcon system) was performed weekly to evaluate the graft attachment, corneal transparency and other pathological changes. The corneal epithelial defects were assessed using

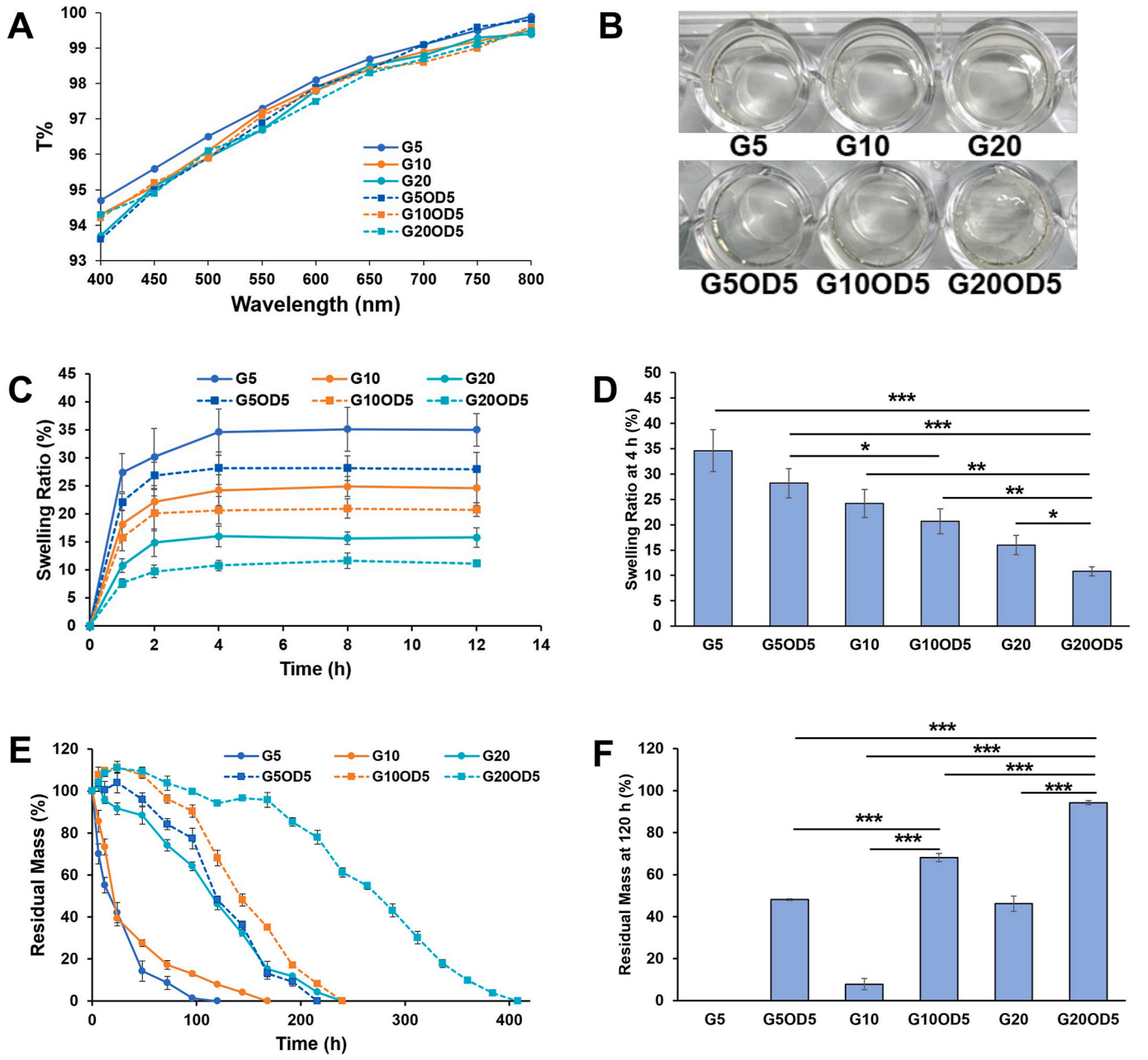

Fig. 2. *In vitro* characterization of the adhesive hydrogels. (A) Light transmission over the visible light spectrum. (B) Gross view of the hydrogels (the thickness of the hydrogel in the well was 100 μm). (C) Swelling ratio at different time points of the hydrogels in PBS at 37 °C. (D) The swelling ratio of the hydrogels after 4 h incubation in PBS at 37 °C. (E) Degradation curve of the hydrogels in the presence of collagenase (1 μg/mL) in PBS at 37 °C. (F) The degradation of the hydrogels after 120 h of incubation in PBS containing 1 μg/mL collagenase. (*P < 0.05, **P < 0.01, ***P < 0.001, n = 3).

fluorescein staining under cobalt blue light. Cross-sectional images of corneal tissue were obtained by spectral-domain AS-OCT (Heidelberg Engineering) to evaluate the graft attachment. *In vivo* confocal microscopy (IVCM, Confoscan 4, Nidek, Japan) was performed under general anesthesia to assess the changes in corneal cells and the status of inflammation. Automatic mode was used to capture images at the levels of the epithelium, anterior stroma and endothelium. The corneal surface curvature flowing sutureless LK was mapped with a corneal tomography system (Optikon 2000, Rome, Italy).

2.10.3. Histological and SEM evaluation of graft integration

Rabbits were sacrificed with an overdose intravenous injection of pentobarbital sodium 8 weeks after surgery. The corneal tissue was excised and processed for routine paraffin embedding. Briefly, 5-μm-thick sections were cut and stained with hematoxylin and eosin (H&E). The paraffin sections were viewed under a light microscope (Axio Imager Z2, Zeiss, Germany). The removed cornea was also prepared for SEM scanning. The samples were first fixed with 2.5% glutaraldehyde for 4 h, followed by three washes in PBS for 15 min each. The samples were then dehydrated by a graded series of ethanol (30%, 50%, 70%, 80%, 90%, 95% and 100%) for 15-20 min each and subjected to SEM examination. Both of the bottom and surrounding graft-recipient interface areas were assessed by histological and SEM examination.

2.11. Statistical analysis

All data were presented as the means ± standard deviation. Comparisons between groups were performed by applying Student's *t*-test

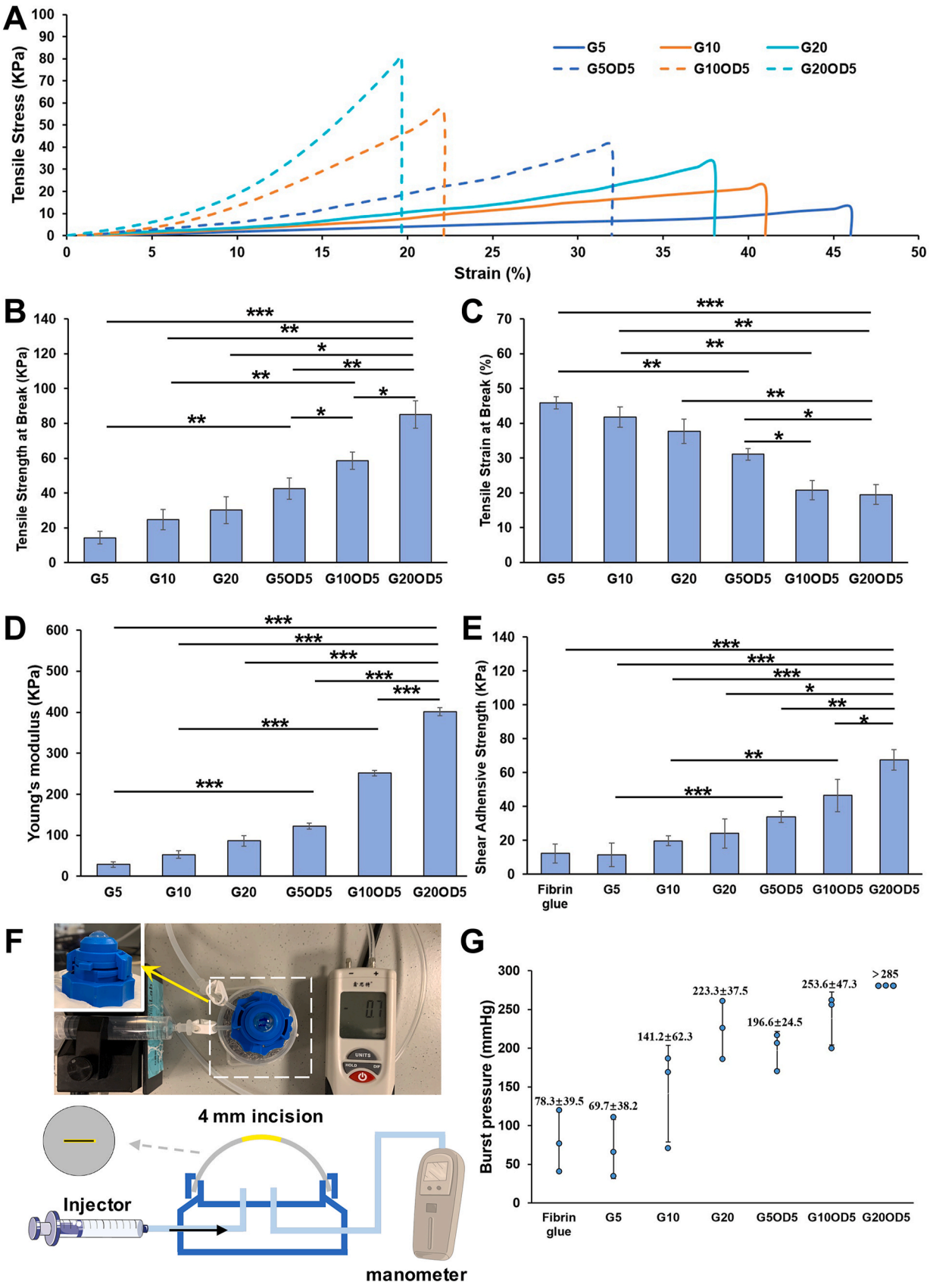

Fig. 3. *In vitro* mechanical properties of hydrogels. (A) Representative tensile stress–strain curves. (B) Tensile strength at break. (C) Tensile strain at break. (D) Young's modulus. (E) Shear adhesive strengths of the adhesive hydrogels compared to fibrin glue. (E) Schematic of *ex vivo* model for burst pressure measurements. (G) Burst pressure. (*P < 0.05, **P < 0.01, ***P < 0.001, n = 3).

using GraphPad Prism 9 (GraphPad Software, USA). A value of $P < 0.05$ was considered statistically significant.

3. Results and discussion

3.1. Fabrication of bioadhesive hydrogels

GelMA hydrogels have recently increased in popularity as tissue sealants due to their suitable biological properties and adjustable physical characteristics [41,42]. GelMA crosslinks and forms hydrogels when exposed to light irradiation. However, pure GelMA hydrogel has poor mechanical strength and adhesive force [43] and cannot replace sutures in corneal transplantation. Therefore, a second interpenetrating network was incorporated into our GelMA-based adhesive hydrogel system to enhance its functionality. ODex is produced by the oxidation of dextran. The oxidation degree of ODex in this study was 103.59 ± 0.31%. The introduction of aldehyde groups in ODex retains the biocompatibility of dextran and enhanced the suitability for chemical modifications. ODex-added adhesives have been reported to be used in lung surgery [44] and amniotic membrane transplantation [45]. The corneal stroma is composed predominantly of collagen, the backbone of which contains abundant amino groups similar to GelMA. Aldehyde groups on ODex can react with these amino groups on GelMA and corneal collagen, and form the first Schiff base network. Light-induced crosslinking later adds the second interpenetrating network to establish double network hydrogels (Fig. 1A). By virtue of the double network structure, hydrogels can achieve sufficient mechanical strength and adhesive force to form a tight bond between the donor graft and the recipient corneal bed [26].

A prehydrogel was prepared by dissolving GelMA and ODex at different ratios in PBS solution. After 10 min of incubation at 37 °C, the prehydrogel solution changed from liquid to solid, but the gelation phenomenon was not observed in GelMA without ODex (Fig. 1B). The gelatinization initiated by the addition of ODex contributes to the formation of the first Schiff base network between the aldehyde groups on ODex and the amino groups on GelMA. Notably, for adhesives, the spontaneous gelation speed should be carefully considered, because if it is too fast, surgeons may not have enough time to properly position the graft. Commercial ocular adhesives such as fibrin glues and cyanoacrylate have been criticized for their short working time [17,18]. However, we found that even the most concentrated GelMA-ODex mix took approximately 5 min to become viscous, which is generally sufficient for careful planning in actual practice. We further confirmed this finding in the following rabbit LK model.

In addition, after we added ODex, the gel system showed a pale-yellow appearance, which may be related to the formation of a Schiff base. Moreover, GelMA hydrogels without ODex also showed a lighter pale-yellow color after solidification, and the colors became deeper as the GelMA concentration increased. Color alteration during gel formation of GelMA has been observed in other studies [46,47]. However, this pale-yellow appearance did not appear to be a major concern. As a tissue adhesive, hydrogel is applied in a thin layer, so such a slight color change would not affect the corneal transparency or visual function.

Many previously reported GelMA adhesives used ultraviolet (UV) light as a trigger [7,41]. However, in this hydrogel system, the second interpenetrating network was formed by photocrosslinking using visible light at a wavelength of 405 nm to prevent ocular damage caused by UV light exposure. We found that all GelMA solutions turned into solid hydrogels regardless of whether ODex was added (Fig. 1B). The photocurability of the material allows temporal and spatial control of the reaction with the assistance of a photoinitiator. From a clinical viewpoint, the greatest advantage of the light-curing adhesive system is that it provides the surgeons with sufficient working time to properly position the graft before using light to gelatinize the adhesive. In this regard, our adhesive hydrogel system exhibits higher controllability for a performance compared to those ocular adhesives that have already been applied in sutureless keratoplasty [18,48].

The microstructure of the hydrogels was further examined with SEM (Fig. 1B). With increasing GelMA concentration and the addition of ODex, the pore size in the hydrogel decreased, indicating a denser structure. The pore size in diameter was approximately 20–100 μm, which is suitable for cell attachment and proliferation [49,50]. Moreover, the pore structure could not only support cell growth, but also facilitate the exchange of nutrients [51], so that the donor graft could obtain nutrients from the recipient tissue when they were applied at the interface.

3.2. Characterization of bioadhesive hydrogels

Adhesives for repairing corneal wounds must be transparent to permit vision [52]. Therefore, the light transmittance of the adhesive hydrogels with different ratios of GelMA to ODex was characterized. According to previous reports, the transmission of the native cornea for light at 430 nm is approximately 80%, but can achieve almost 100% for light at 500 nm and above [53]. As shown in Fig. 2A, the light transmittance of the adhesive hydrogels was above 90% in the visible light range (wavelength of 400 nm–800 nm) and close to 100% at wavelength of 800 nm. Our findings indicated that all the tested hydrogels exhibited comparable or superior light transmittance to that of native corneas. In addition, we have discussed above that the yellow transition during hydrogel gelation was not a major issue when it was applied in a thin layer. Here, Fig. 2B also showed that the photocrosslinked hydrogels were optically clear and colorless when they were formed a layer in the well with a thickness of approximately 100 μm. This thickness is already far thicker than that in actual applications.

The swelling rate is a crucial indicator to judge the advantages and disadvantages of tissue adhesives. A lower swelling rate is beneficial for tissue bonding purposes. In terms of application in keratoplasty, adhesive with a low swelling rate can help to maintain perfect alignment between the graft and recipient cornea, and therefore, reduce the postoperative corneal astigmatism. Our results showed that the concentration of GelMA and the addition of ODex could directly affect the swelling rate (Fig. 2C–D). With an increasing GelMA concentration and the introduction of ODex, the swelling rate of the hydrogels decreased and reached equilibrium after 4 h. G5 was found to have the highest swelling rate (35.01 ± 2.89%), while G20OD5 had the lowest swelling rate (11.19 ± 0.59%). Compact materials absorb less water and have a lower swelling rate. Therefore, the reduced swelling rate after the introduction of the ODex should be attributed to the higher network density and degree of cross-linking.

One of the reasons why fibrin glues are not popular in keratoplasty is that they are prone to degradation, which would increase the risk of graft loss [54]. In this study, adhesive hydrogels with different compositions of GelMA and ODex were tested for their enzymatic degradation by collagenase. As presented in Fig. 2E–F, the enzymatic resistance of hydrogels was improved with increasing GelMA concentration and the introduction of ODex, which is similar to swelling rate trend. The degradation time of G5 was the shortest (approximately 120 h), while that of G20OD5 was the longest (approximately 400 h). This trend is easily explained by the increased degree of crosslinking. Moreover, the residual masses of G5OD5, G10OD5 and G20OD5 exceeded their original mass during the initial stage of degradation process. This finding may be because that prior to digestion by collagenases, the hydrogels swell as crosslinks are hydrolyzed [55].

The mechanical strength and adhesive force are the most critical metrics for adhesives [56]. In terms of use in corneal transplantation, adhesives should provide sufficient adhesive force to be able to bear the intraocular pressure (IOP)-related stress. Otherwise, improper juxtaposition of wound edges or even graft loss may occur. First, we characterized the tensile strength, elongation at break, and Young's modulus of the hydrogels with different polymer concentrations. Fig. 3A shows the stress-strain curve of the hydrogels. According to the quantitative

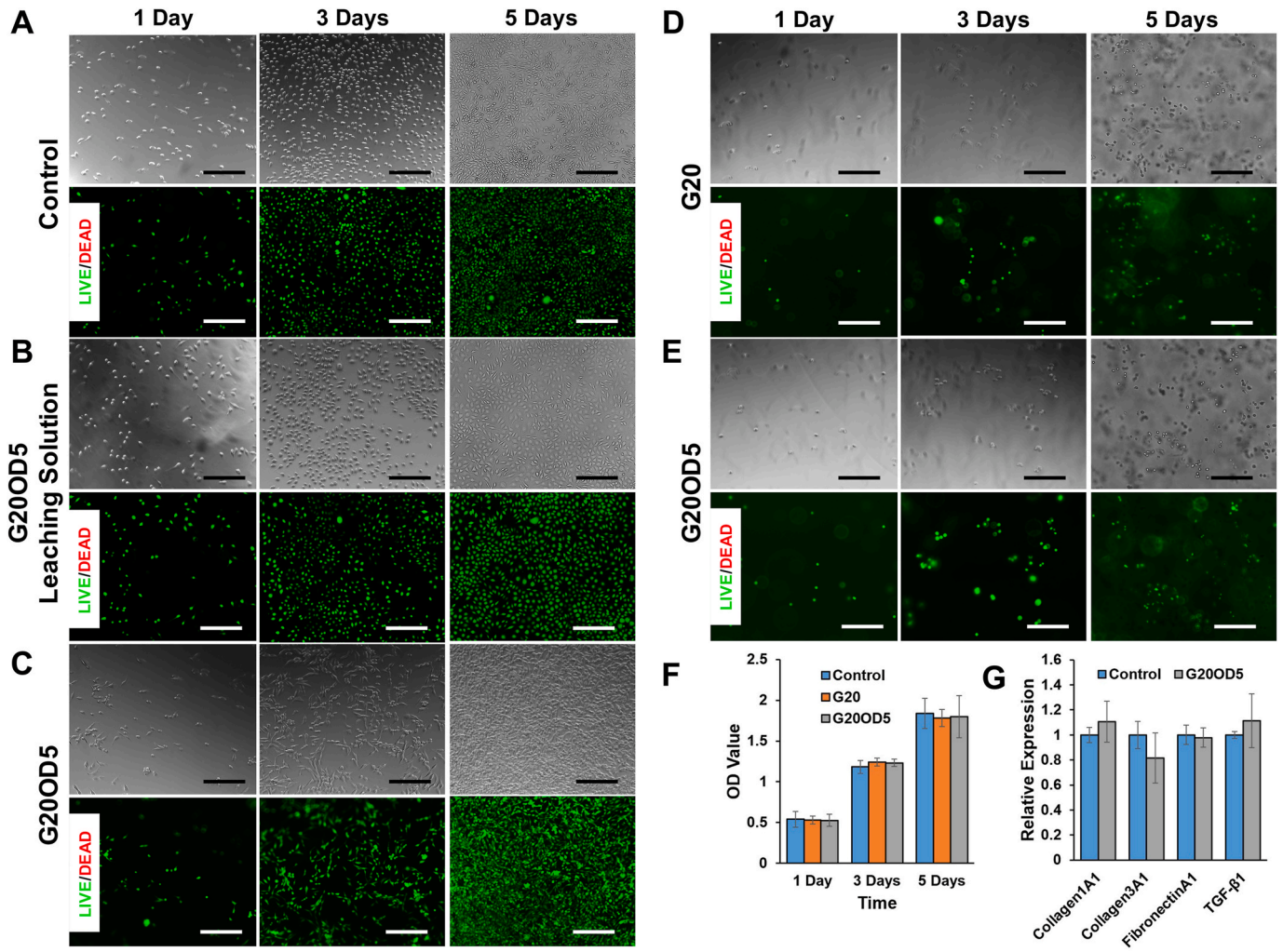

Fig. 4. *In vitro* cytocompatibility assessments of the adhesive hydrogels. Representative bright field and live-dead images of L929 cells that were seeded on tissue culture plates in complete medium (A) and G20OD5 leaching medium (B), on the surface of the G20OD5 hydrogel (C), and encapsulated in G20 (D) and G20OD5 hydrogels (E). (F) CCK-8 assay of cells cultured in complete medium, and G20 and G20OD5 leaching medium after 1, 3, and 5 days of seeding. (G) qRT-PCR analysis of the relative mRNA expression levels of Collagen 1A1, Collagen 3A1, Fibronectin A1 and TGF-β1 mRNA in rabbit corneal fibroblasts after culture in complete medium and G20OD5 leaching medium for 2 days. Scale bar: 100 μm.

measurements of maximum tensile strength (Fig. 3B) and breaking elongation (Fig. 3C), it can be seen that G20OD5 had the highest tensile strength (85.07 ± 7.91 KPa) and the lowest elongation at break (19.49 ± 2.80%). This finding is also because G20OD5 had the highest GelMA concentration and degree of crosslinking. Due to the high tensile strength and low elongation at break, G20OD5 had the highest Young's modulus (Fig. 3D), indicating that it has the best elasticity and resistance to deformation.

Next, we characterized the adhesive strength of the hydrogels. Given that the bonding force mainly relies on the adhesion between the interface of the donor graft and recipient bed, we thus characterized the shear adhesive strength of the hydrogels compared to that of commercial adhesive fibrin. It can be seen from Fig. 3E that the shear adhesive strength of fibrin glue was relatively low (12.20 ± 5.62 kPa). With increasing GelMA concentration and the introduction of ODex, the shear adhesive strength of the hydrogel was substantially improved. G20OD5 showed the best shear adhesive strength (67.52 ± 6.12 kPa). The Schiff's base and hydrogel bonds between the hydrogel and tissue contribute to the strong tissue adhesion [57]. Therefore, firstly, the abundance of hydrogen bonds is one of the reasons for the greater adhesive strength of G20OD5. An increase of GelMA concentration would introduce more functional groups to the hydrogels, which can form more hydrogen bonds with the hydroxyl, carboxyl and amino groups of the tissue, and thereby results in higher adhesive strength. That increased GelMA concentration leads to better adhesive strength has also been reported in the previous study [39]. Secondly, ODex introduces Schiff's base between materials and tissues, thereby providing the hydrogel with good bonding ability. Theoretically, an increase of ODex concentration can improve the adhesive strength of hydrogels by forming more Schiff's bases. The shear adhesive strength of hydrogels with various ODex concentrations (2.5%, 5% and 10% (w/v)) has been compared in our preliminary study. The adhesive strength was found to be weak at lower ODex concentration (2.5%). A stronger adhesive strength was observed at higher ODex concentration. However, hydrogels with 10% ODex underwent fast gelatinization even without light irritation. This would pose challenges for use in keratoplasty. Based on this consideration, ODex concentration of 5% was chosen for the *in vitro* and *in vivo* assessments in this study.

The adhesion characteristics of the hydrogels was further tested using a previously described *ex-vivo* model (Fig. 3F) [25,39]. The results showed that G20OD5 had the strongest adhesive strengthen and was able to withstand an IOP greater than 280 mmHg (Fig. 3G). This is approximately 10 times higher than that of normal IOP. These findings indicated that our adhesive hydrogel may theoretically be able to withstand the postoperative increased IOP in most instances. However, many patients' behavior, such as eye rubbing and Valsalva maneuvers,

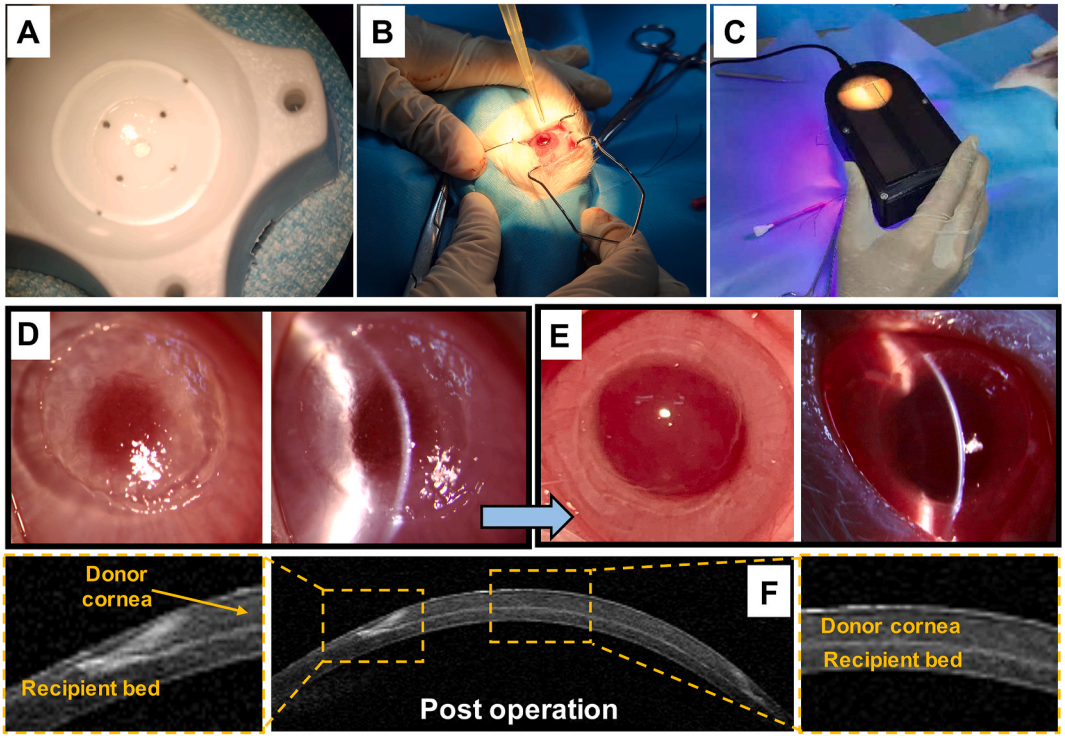

Fig. 5. *In vivo* evaluation of the G20OD5 adhesive hydrogel in a rabbit model of lamellar keratoplasty. (A) Representative images of the donor cornea. (B) Application of G20OD5 prepolymer solution to the surface of recipient corneal bed. (C) Photocrosslinking after the donor cornea was transferred to the recipient corneal bed and adjusted to the proper position. Slit lamp photographs before (D) and after (E) sutureless lamellar keratoplasty using the G20OD5 adhesive hydrogel. (F) Anterior segment optical coherence tomography (AS-OCT) images of the operated cornea following sutureless lamellar keratoplasty using the G20OD5 adhesive hydrogel.

can result in spikes in IOP. Wound leak may occur under extreme spikes of IOP, even in the setting of keratoplasty using sutures as the bounding method. Therefore, patients should be educated to avoid any behavior that may increase IOP, especially at the initial postoperative period.

3.3. *In vitro assessment of cytocompatibility*

G20OD5 had the most favorable physical properties and hence was subjected for further cytocompatibility testing. Both 2-D and 3-D culture systems were employed in these *in vitro* studies. Cell culture-treated plates (Fig. 4A) and noncytotoxic pure GelMA (G20, Fig. 4D) hydrogel were functioned as negative controls for 2-D and 3-D culture systems, respectively. Whenever they were cultured in medium leached from G20OD5 (Fig. 4B), on the surface of the light-cured G20OD5 hydrogel (Fig. 4C) or encapsulated in the G20OD5 hydrogel (Fig. 4E), L929 cells did not show apparent differences in cell growth compared to their negative controls. In addition, live/dead staining was carried out to evaluate the effects of the G20OD5 hydrogel system on L929 viability. We found that cells in all the above-mentioned culture conditions exhibited high viability 1, 3 and 5 days after seeding, and almost no dead cells were detectable. A CCK-8 kit was further employed to investigate the cytotoxicity of G20OD5 hydrogels. The CCK-8 test results showed that exposure of L929 cells to the leaching medium of G20OD5 did not cause a reduction in cell viability (Fig. 4F).

In response to infections, injuries and surgeries, quiescent corneal keratocytes transform into contractile and opaque myofibroblasts, resulting in the secretion of disordered extracellular matrix and corneal scar formation [58]. Prevention of this transformation process favors corneal wound healing without scarring. Therefore, we tested the expression of the myofibroblast-related genes Collagen 1A1, Collagen 3A1, Fibronectin A1 and TGF-β1 to characterize the myofibroblast transformation following G20OD5 application. Our results did not show any excess myofibroblast transformation when the cells were cultured in G20OD5 leached medium, indicating that the use of G20OD5 in keratoplasty would not lead to excess scar formation (Fig. 4G).

3.4. *In vivo assessment of G20OD5 in rabbit sutureless LK*

Because our *in vitro* mechanical assessment showed that G20OD5 had the strongest adhesive strength, herein, it was used to investigate the adhesive performance in the New Zealand rabbit model of corneal lamellar transplant. First, we prepared a donor corneal graft with a diameter of 7 mm and a thickness of approximately 200 μm (Fig. 5A). After a recipient stromal bed with the desired depth was created using a trephine 0.25 mm less in size than the donor, the prehydrogel liquid of G20OD5 was applied to the cut surface of the bed (Fig. 5B). The donor graft was then immediately transferred onto the recipient bed in the proper position, followed by in situ photocrosslinking via visible light for 4 min (Fig. 5C). An Elizabeth collar was used after the operation to prevent the rabbits from scratching their eyes. Fig. 5D showed the two-thirds thickness corneal stroma defect created in the study. G20OD5 had adequate adhesive strength that was derived from its two internal crosslinked networks. After application of G20OD5 followed by photocrosslinking, the donor graft was firmly attached to the recipient bed (Fig. 5E). As we showed above, although G20OD5 appeared very light pale-yellow, we found that when it was applied as a thin layer in LK, the pale-yellow appearance was not detected and did not affect its light transmission. The operated cornea had good optical transparency under slit-lamp microscopy. Cross-sectional AS-OCT images further showed the perfect fit between the donor and host corneas (Fig. 5F).

An ideal ocular adhesive for corneal transplantation should also allow sufficient handling time before it was completely set in situ [18]. To provide increased adhesive strength, a secondary covalent network was incorporated into our adhesion system by adding ODex. Upon the mixture of two components, the first Schiff based network starts to form before photocrosslinking, which resulted in the initiation of

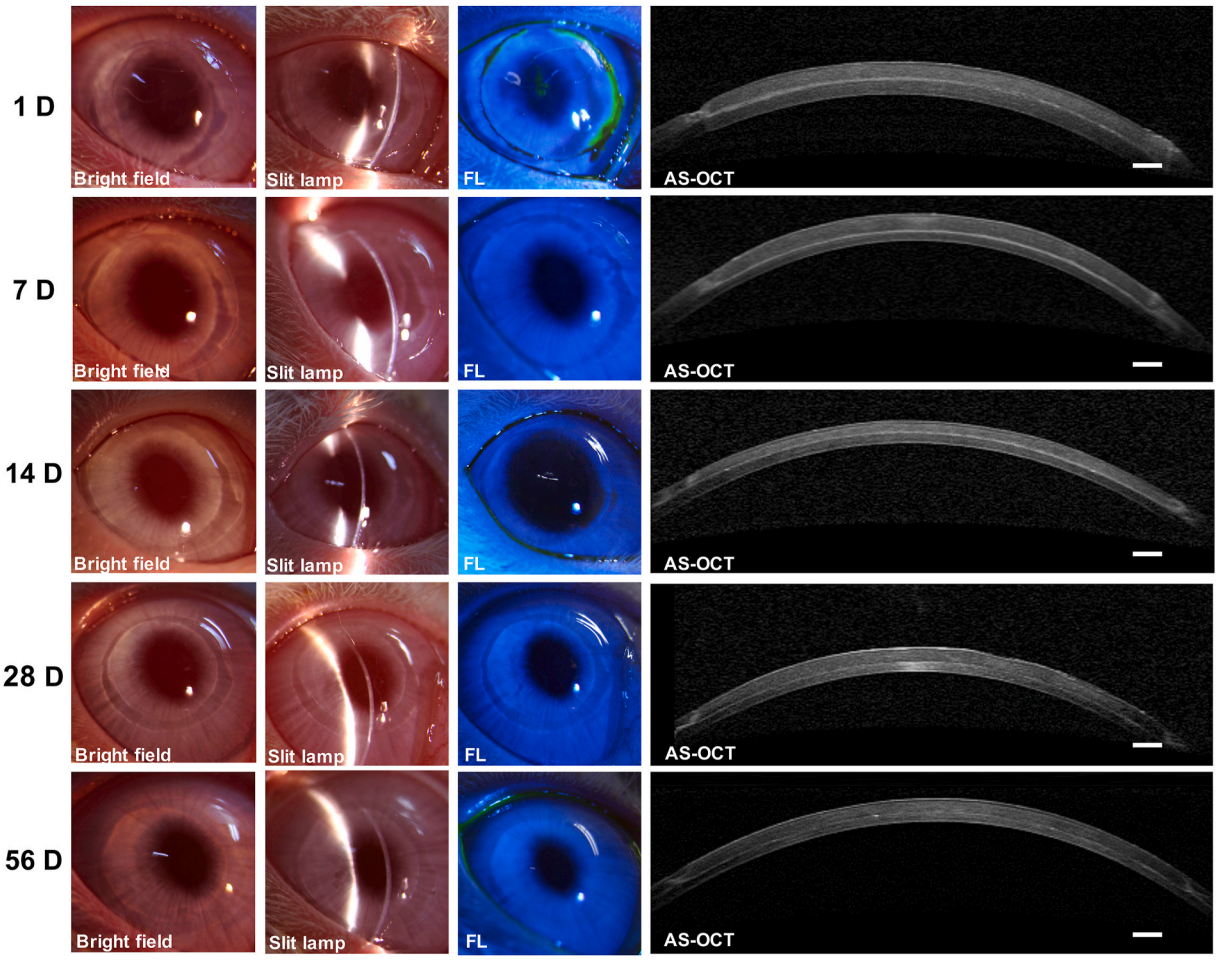

Fig. 6. Postoperative observation using slit-lamp microscopy and anterior segment optical coherence tomography (AS-OCT). Representative slit-lamp and AS-OCT images of rabbit corneas taken 1, 7, 14, 28 and 56 days after sutureless keratoplasty. Scale bar: 400 μm.

gelatinization. Gelatinization would bring challenges for graft manipulation. Therefore, the gelatinization time of bioadhesives should be adjusted beforehand to ensure convenience in practical applications. We found that G20OD5 had an appropriate gel formation time to ensure that the surgeons had adequate time to carefully adjust the graft in the proper position. This advantage could just compensate for one of the deficiencies of cyanoacrylate and fibrin glue. The later materials were reported to have a short working time for careful planning [4]. The adhesive strength is proportional to the concentration of components. Therefore, although G20OD5 is wet-tolerant, the excess fluid on the corneal surface tends to reduce the concentration of components, resulting in a longer gelatinization time and weaker adhesive strength.

The main requirement for a bioadhesive is its bonding strength. The use of fibrin glue without sutures for LK has been reported [17,18]. However, this material has not gained popularity in corneal transplantation since its first report in the 2000s because of low adhesive strength and rapid degradation. In this study, we found that the G20OD5 adhesive could overcome for these shortcomings and provide satisfactory attachment for LK. As shown in Fig. 6, the graft was firmly attached without loosening and dislocation throughout the experimental period. The cornea preserved a smooth surface and complete curve. There was no visible scar and epithelial ingrowth on the donor-host interface. The donor graft and recipient cornea remained transparent without excessive inflammation, although a slight corneal edema was observed only at the initial postoperative period. In addition, the G20OD5 adhesive allowed quick regeneration of corneal epithelial cells after the operation. Fluorescein staining revealed that the corneal epithelial defects were confined to the junction of graft and recipient cornea 1 day after the operation. They were completely healed by postoperative day 7.

Scarring at the interface would affect the vision outcomes after LK [59]. On the AS-OCT images of post-LK cornea, there is always a dividing line at the interface because of inevitable interface haze. During the initial postoperative period, the thick dividing lines between the graft and the recipient cornea on our AS-OCT images were quite possibly because of the hydrogel accumulation rather than the interface haze. But excessive adhesive buildup at the interface was not observed. The bioadhesive formed a thin layer in-between. An ideal bioadhesive should be biodegradable on a time scale consistent with wound healing. The AS-OCT examination further showed that the dividing line between the graft and the recipient corneal bed became increasingly undetectable, indicating the eventual degradation of G20OD5 and scarless wound healing. However, for the application of bioadhesives in LK, rapid degradation, such as that of fibrin glue, is also not favored, given that the risk of graft dislocation or even less would be increased. This issue should not be a problem in double-network hydrogels such as G20OD5, given their resistance to collagenase. Moreover, in combination with the data of above *in vitro* cell assessments, the invisible dividing line also further supports that the adhesive hydrogel at the interface would not cause additional interface haze. However, the interface haze formation in the long-term still needs to be further evaluated and compared to that of LK techniques using sutures.

IVCM was used to further confirm the biocompatibility of the G20OD5 adhesive *in vivo*. By 56 days after surgery, no epithelial, stromal or endothelial cell abnormalities were observed in the operated cornea

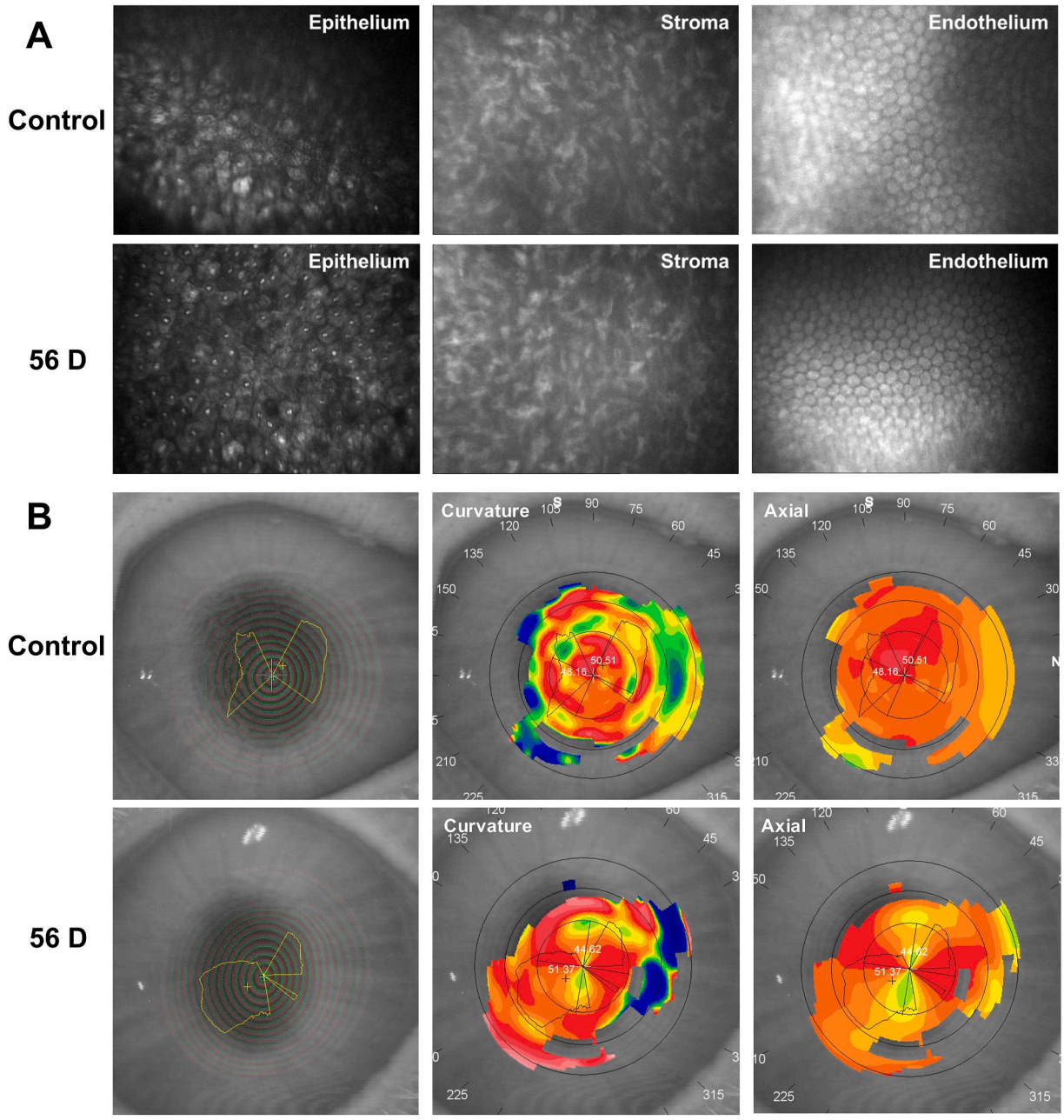

Fig. 7. Postoperative observation by *in vivo* confocal microscopy (A) and corneal topography (B) of the native rabbit cornea and the operated rabbit corneas 56 days after sutureless lamellar keratoplasty. Scale bar: up: 200 μm, down: 50 μm.

(Fig. 7A). Inflammatory cells and necrotic debris were characterized by the presence of hyperreflective punctuate foci, and corneal stromal scarring is visible as a hyperreflective bright white region on IVCM scans. These abnormalities were also not observed in the operated cornea, indicating that the cornea following G20OD5 application remained transparent and noninflamed. The use of bioadhesive for graft attachment avoids the need for sutures, and the latter can induce irregular astigmatism and distort optics [3]. The corneal topography was thus evaluated. The results showed moderate but still symmetrical corneal curvature changes in the operated cornea compared to those in the control cornea (Fig. 7B).

Moreover, histological examinations of cryosectioned tissues further revealed that the transplanted graft was well attached to the recipient corneal bed without any gaps or debris in the interface (Fig. 8A). One of the reported potential advantages of sutureless corneal surgery using bioadhesives includes reducing the possibility of postoperative epithelial ingrowth beneath flaps and grafts [60]. Our histological evaluation did not show any epithelial ingrowth into the interface from the edge. The stroma proximal to the interface appeared normal. Inflammatory cell infiltration and apparent scarring were also not observed in histological images. The corneal epithelium over the graft was well stratified and differentiated, which were similar to that in the control cornea. Electron microscopic assessment showed that the donor graft was closely adhered to the recipient corneal bed, including at the bottom and surrounding graft-host interface (Fig. 8B). The adhesive hydrogel layer was also found to almost completely disappeared from the interface, further indicating that G20OD5 could eventually degrade after the wound healed. All these findings suggest that the G20OD5 adhesive system has good *in vivo* biocompatibility and supports native tissue repair.

It is worth to note that the partial thickness LK model used in this study does not quite mimic the DALK that is performed in humans. The

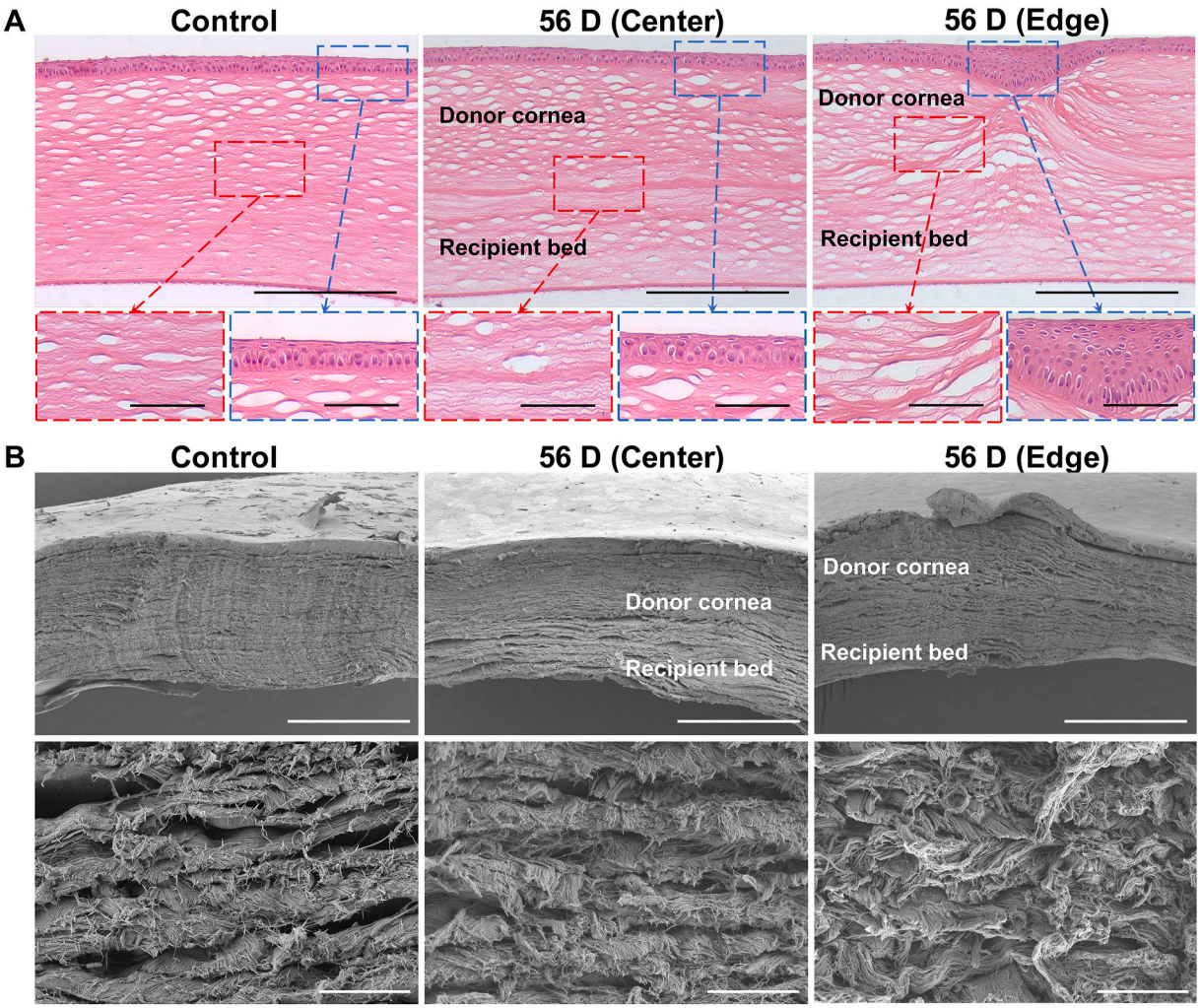

Fig. 8. Representative hematoxylin–eosin (HE) and scanning electron microscope (SEM) images of native rabbit corneas or and the operated rabbit corneas 56 days after sutureless lamellar keratoplasty. Both of the bottom and surrounding graft-recipient interface areas were evaluated. Scale bar in A: up: 200 μm, down: 50 μm. Scale bar in B: up: 200 μm, down: 10 μm.

reason why DALK model was not used for assessment is that it is technically difficult to perform DALK on rabbit cornea. Probably for the same reason, DALK was also rarely performed on rabbit in the related published studies [61–64]. The adhesive hydrogel is closer to corneal endothelium if used for DALK. However, there is theoretically no need to be worried that it may bring toxicity to endothelium, because the GelMA-based hydrogel is characterized by excellent biocompatibility and low immune response [42]. Our *in vitro* assessment has also showed that the G20OD5 adhesive hydrogel did not affect cell proliferation or viability. Moreover, G20OD5 hydrogel was found to have a burst pressure that is approximately 10 times higher than that of normal IOP. Taken all of this evidence together, although the feasibility has not been tested in DALK model, our adhesive hydrogel theoretically should have reasonable safety and sufficient adhesive strength for DALK. However, the safety and efficiency of this adhesive system still needs to be further evaluated *in vivo* using DALK animal model before it is applied in humans. Penetrating keratoplasty (PKP) refers as a full-thickness transplant of the diseased cornea with a donor cornea [65]. In spite of wet-tolerance, our adhesive hydrogels are not recommendable for PK, as they might be diluted by the aqueous humor, thereby resulting in reducing the adhesive strength.

Our 8-week follow-up period was admittedly short, given that sutures are generally removed 12 months after keratoplasty in clinical practice. However, they seemed to be removed much earlier in animal studies than those in humans. In several studies using rabbit LK model, sutures were removed 30 days after operation, and no graft loss or dislocation was noted [48,66]. Moreover, a previous study indicated that in terms of sutureless keratoplasty using glue as the bonding method, the glue was only required to anchor the donor cornea until complete re-epithelialization [17]. In our study, on one hand, we found that G20OD5 adhesive hydrogel allowed quick regeneration of corneal epithelial cells and that the graft epithelial defects healed within one week after transplantation; on the other hand, although we did observe the signs of hydrogel degradation in the follow-up time frame, this degradation process is very slow due to its resistance to collagenase digestion. Therefore, our adhesive hydrogel should have sufficient mechanical and adhesive strength to retain the donor cornea in place until graft re-epithelialization is complete.

4. Conclusion

In summary, the use of sutures in keratoplasty is not only time consuming, but also associated with multiple postoperative complications. To resolve this issue, we have developed a photocurable bioadhesive hydrogel composed of GelMA and ODex to avoid the need for sutures in keratoplasty. This hydrogel has the characteristics of ideal corneal adhesives, including high light transmittance, resistance to enzymatic degradation and excellent biocompatibility. Moreover, by

virtue of the double network structure, our bioadhesive hydrogel exhibits superior adhesive strength in compared to commercial fibrin glues, and has the capacity to bond the graft to the recipient corneal bed until the wound heals. Following application, this system supports the graft-recipient corneal integration by eventual degradation, and the corneas remain transparent and uninflamed, further indicating its acceptable compatibility. In addition, from the viewpoint of convenience of operation, the photocurable properties of this adhesive hydrogel provide sufficient working time to surgeons for careful planning. Thus, this bioadhesive hydrogel may be an appealing option as a suture substitute in keratoplasty, cornea injury repair and other procedures involving tissue adhesion.

Author contributions statement

X. Zhao designed the study, performed the *in vitro* experiments, helped with the *in vivo* experiments and wrote the paper. S. Li designed the study, performed the *in vivo* experiments, helped with the *in vitro* experiments, and wrote and revised the paper. X. Du helped with the *in vitro* and *in vivo* experiments. W. Li performed the *in vivo* experiments. Q. Wang helped with the *in vivo* experiments. D. He helped with the *in vitro* experiments. J. Yuan conceived, designed the experiment and revised the paper.

CRediT authorship contribution statement

Xuan Zhao: Conceptualization, Methodology, Validation, Investigation, Writing – original draft, Visualization. **Saiqun Li:** Conceptualization, Methodology, Formal analysis, Investigation, Writing – review & editing, Visualization. **Xinyue Du:** Validation, Investigation. **Weihua Li:** Resources, Investigation. **Qian Wang:** Investigation. **Dalian He:** Validation. **Jin Yuan:** Conceptualization, Supervision, Project administration, Funding acquisition.

Declaration of competing interest

There are no conflicts of interest in this work.

Acknowledgements

This research has been supported by National Natural Science Foundation of China (81870633) and Guangdong Province Key Field R&D Program (2020B1111150002).

References

[1] S.R. Flaxman, R.R.A. Bourne, S. Resnikoff, P. Ackland, T. Braithwaite, M. V. Cicinelli, A. Das, J.B. Jonas, J. Keeffe, J.H. Kempen, J. Leasher, H. Limburg, K. Naidoo, K. Pesudovs, A. Silvester, G.A. Stevens, N. Tahhan, T.Y. Wong, H. R. Taylor, S. Vision Loss Expert Group of the Global Burden of Disease, Global causes of blindness and distance vision impairment 1990-2020: a systematic review and meta-analysis, Lancet Glob Health 5 (12) (2017) e1221–e1234.

[2] P. Gain, R. Jullienne, Z. He, M. Aldossary, S. Acquart, F. Cognasse, G. Thuret, Global survey of corneal transplantation and eye banking, JAMA Ophthalmol 134 (2) (2016) 167–173.

[3] A.Z. Crawford, J.J. Meyer, D.V. Patel, S.E. Ormonde, C. McGhee, Complications related to sutures following penetrating and deep anterior lamellar keratoplasty, Clin. Exp. Ophthalmol. 44 (2) (2016) 142–143.

[4] G. Trujillo-de Santiago, R. Sharifi, K. Yue, E.S. Sani, S.S. Kashaf, M.M. Alvarez, J. Leijten, A. Khademhosseini, R. Dana, N. Annabi, Ocular adhesives: design, chemistry, crosslinking mechanisms, and applications, Biomaterials 197 (2019) 345–367.

[5] Y. Gao, Y. Han, M. Cui, H.L. Tey, L. Wang, C. Xu, ZnO nanoparticles as an antimicrobial tissue adhesive for skin wound closure, J. Mater. Chem. B 5 (23) (2017) 4535–4541.

[6] B. Hoffmann, E. Volkmer, A. Kokott, P. Augat, M. Ohnmacht, N. Sedlmayr, M. Schieker, L. Claes, W. Mutschler, G. Ziegler, Characterisation of a new bioadhesive system based on polysaccharides with the potential to be used as bone glue, J. Mater. Sci. Mater. Med. 20 (10) (2009) 2001–2009.

[7] Y. Hong, F. Zhou, Y. Hua, X. Zhang, C. Ni, D. Pan, Y. Zhang, D. Jiang, L. Yang, Q. Lin, Y. Zou, D. Yu, D.E. Arnot, X. Zou, L. Zhu, S. Zhang, H. Ouyang, A strongly adhesive hemostatic hydrogel for the repair of arterial and heart bleeds, Nat. Commun. 10 (1) (2019) 2060.

[8] S. Bloomfield, A.H. Barnert, P. Kanter, The use of Eastman-910 monomer as an adhesive in ocular surgery. II. Effectiveness in closure of limbal wounds in rabbits, Am. J. Ophthalmol. 55 (1963) 946–953.

[9] S. Masket, J.A. Hovanesian, J. Levenson, F. Tyson, W. Flynn, M. Endl, P. A. Majmudar, S. Modi, R. Chu, M.B. Raizman, S.S. Lane, T. Kim, Hydrogel sealant versus sutures to prevent fluid egress after cataract surgery, J. Cataract Refract. Surg. 40 (12) (2014) 2057–2066.

[10] S. Srinivasan, M. Dollin, P. McAllum, Y. Berger, D.S. Rootman, A.R. Slomovic, Fibrin glue versus sutures for attaching the conjunctival autograft in pterygium surgery: a prospective observer masked clinical trial, Br. J. Ophthalmol. 93 (2) (2009) 215–218.

[11] D. Miki, K. Dastgheib, T. Kim, A. Pfister-Serres, K.A. Smeds, M. Inoue, D. L. Hatchell, M.W. Grinstaff, A photopolymerized sealant for corneal lacerations, Cornea 21 (4) (2002) 393–399.

[12] S. Guhan, S.L. Peng, H. Janbatian, S. Saadeh, S. Greenstein, F. Al Bahrani, A. Fadlallah, T.C. Yeh, S.A. Melki, Surgical adhesives in ophthalmology: history and current trends, Br. J. Ophthalmol. 102 (10) (2018) 1328–1335.

[13] C. Scalcione, D. Ortiz-Vaquerizas, D.G. Said, H.S. Dua, Fibrin glue as agent for sealing corneal and conjunctival wound leaks, Eye 32 (2) (2018) 463–466.

[14] A. Sharma, R. Kaur, S. Kumar, P. Gupta, S. Pandav, B. Patnaik, A. Gupta, Fibrin glue versus N-butyl-2-cyanoacrylate in corneal perforations, Ophthalmology 110 (2) (2003) 291–298.

[15] J.D. Harvey, R.L. Gross, B.D. McMillan, Novel use of fibrin sealant for scleral suture free placement of a glaucoma drainage device in advanced scleral thinning, Am J Ophthalmol Case Rep 9 (2018) 7–9.

[16] P. Rama, S. Bonini, A. Lambiase, O. Golisano, P. Paterna, M. De Luca, G. Pellegrini, Autologous fibrin-cultured limbal stem cells permanently restore the corneal surface of patients with total limbal stem cell deficiency, Transplantation 72 (9) (2001) 1478–1485.

[17] H. Hashemi, A. Dadgostar, Automated lamellar therapeutic keratoplasty with fibrin adhesive in the treatment of anterior corneal opacities, Cornea 30 (6) (2011) 655–659.

[18] H.E. Kaufman, M.S. Insler, H.A. Ibrahim-Elzembely, S.C. Kaufman, Human fibrin tissue adhesive for sutureless lamellar keratoplasty and scleral patch adhesion: a pilot study, Ophthalmology 110 (11) (2003) 2168–2172.

[19] F. Luengo-Gimeno, D.T. Tan, J.S. Mehta, Evolution of deep anterior lamellar keratoplasty (DALK), Ocul. Surf. 9 (2) (2011) 98–110.

[20] M. Hino, O. Ishiko, K.I. Honda, T. Yamane, K. Ohta, T. Takubo, N. Tatsumi, Transmission of symptomatic parvovirus B19 infection by fibrin sealant used during surgery, Br. J. Haematol. 108 (1) (2000) 194–195.

[21] M. Kawamura, M. Sawafuji, M. Watanabe, H. Horinouchi, K. Kobayashi, Frequency of transmission of human parvovirus B19 infection by fibrin sealant used during thoracic surgery, Ann. Thorac. Surg. 73 (4) (2002) 1098–1100.

[22] T.M.D. Le, H.T.T. Duong, T. Thambi, V.H. Giang Phan, J.H. Jeong, D.S. Lee, Bioinspired pH- and temperature-responsive injectable Adhesive hydrogels with polyplexes promotes skin wound healing, Biomacromolecules 19 (8) (2018) 3536–3548.

[23] Y. Liu, Z. Zhu, X. Pei, X. Zhang, X. Cheng, S. Hu, X. Gao, J. Wang, J. Chen, Q. Wan, ZIF-8-Modified multifunctional bone-adhesive hydrogels promoting angiogenesis and osteogenesis for bone regeneration, ACS Appl. Mater. Interfaces 12 (33) (2020) 36978–36995.

[24] A.M. Oelker, J.A. Berlin, M. Wathier, M.W. Grinstaff, Synthesis and characterization of dendron cross-linked PEG hydrogels as corneal adhesives, Biomacromolecules 12 (5) (2011) 1658–1665.

[25] E. Shirzaei Sani, A. Kheirkhah, D. Rana, Z. Sun, W. Foulsham, A. Sheikhi, A. Khademhosseini, R. Dana, N. Annabi, Sutureless repair of corneal injuries using naturally derived bioadhesive hydrogels, Sci Adv 5 (3) (2019), eaav1281.

[26] A.P. Dhand, J.H. Galarraga, J.A. Burdick, Enhancing Biopolymer Hydrogel Functionality through Interpenetrating Networks, Trends in Biotechnology 39 (5) (2021) 519–538, https://doi.org/10.1016/j.tibtech.2020.08.007. ISSN: 0167-7799.

[27] B.R. Freedman, O. Uzun, N.M.M. Luna, A. Rock, C. Clifford, E. Stoler, G. Östlund-Sholars, C. Johnson, D.J. Mooney, Degradable and removable tough adhesive hydrogels, Adv. Mater. (2021), e2008553.

[28] W. Zhu, Y.J. Chuah, D.A. Wang, Bioadhesives for internal medical applications: a review, Acta Biomater. 74 (2018) 1–16.

[29] J.P. Gong, Y. Katsuyama, T. Kurokawa, Y. Osada, Double-network hydrogels with extremely high mechanical strength, Adv. Mater. 15 (14) (2003) 1155–1158.

[30] L. Wang, X. Zhang, K. Yang, Y.V. Fu, T. Xu, S. Li, D. Zhang, L.N. Wang, C.S. Lee, A novel double-crosslinking-double-network design for injectable hydrogels with enhanced tissue adhesion and antibacterial capability for wound treatment, Adv. Funct. Mater. 30 (1) (2020), 1904156.

[31] C.S. Russell, A. Mostafavi, J.P. Quint, A.C. Panayi, K. Baldino, T.J. Williams, J. G. Daubendiek, V. Hugo Sánchez, Z. Bonick, M. Trujillo-Miranda, In situ printing of adhesive hydrogel scaffolds for the treatment of skeletal muscle injuries, ACS Appl. Bio Mater. 3 (3) (2020) 1568–1579.

[32] N. Rajabi, M. Kharaziha, R. Emadi, A. Zarrabi, H. Mokhtari, S. Salehi, An adhesive and injectable nanocomposite hydrogel of thiolated gelatin/gelatin methacrylate/Laponite(R) as a potential surgical sealant, J. Colloid Interface Sci. 564 (2020) 155–169.

[33] D. Gan, Z. Wang, C. Xie, X. Wang, W. Xing, X. Ge, H. Yuan, K. Wang, H. Tan, X. Lu, Mussel-inspired tough hydrogel with in situ nanohydroxyapatite mineralization for osteochondral defect repair, Adv Healthc Mater 8 (22) (2019), e1901103.

[34] H. Zhang, A. Qadeer, D. Mynarcik, W. Chen, Delivery of rosiglitazone from an injectable triple interpenetrating network hydrogel composed of naturally derived materials, Biomaterials 32 (3) (2011) 890–898.
[35] H. Zhao, N.D. Heindel, Determination of degree of substitution of formyl groups in polyaldehyde dextran by the hydroxylamine hydrochloride method, Pharm. Res. (N. Y.) 8 (3) (1991) 400–402.
[36] Y. Liu, L. Ren, K. Long, L. Wang, Y. Wang, Preparation and characterization of a novel tobramycin-containing antibacterial collagen film for corneal tissue engineering, Acta Biomater. 10 (1) (2014) 289–299.
[37] C. Deng, F. Li, J.M. Hackett, S.H. Chaudhry, F.N. Toll, B. Toye, W. Hodge, M. Griffith, Collagen and glycopolymer based hydrogel for potential corneal application, Acta Biomater. 6 (1) (2010) 187–194.
[38] M. Tavafoghi, A. Sheikhi, R. Tutar, J. Jahangiry, A. Baidya, R. Haghniaz, A. Khademhosseini, Engineering tough, injectable, naturally derived, bioadhesive composite hydrogels, Adv Healthc Mater 9 (10) (2020), e1901722.
[39] A. Barak, O. Eyal, M. Rosner, E. Belotserkousky, A. Solomon, M. Belkin, A. Katzir, Temperature-controlled CO2 laser tissue welding of ocular tissues, Surv. Ophthalmol. 42 (Suppl 1) (1997) S77–S81.
[40] H. Mishima, K. Yasumoto, T. Nishida, T. Otori, Fibronectin enhances the phagocytic activity of cultured rabbit keratocytes, Invest. Ophthalmol. Vis. Sci. 28 (9) (1987) 1521–1526.
[41] A. Assmann, A. Vegh, M. Ghasemi-Rad, S. Bagherifard, G. Cheng, E.S. Sani, G. U. Ruiz-Esparza, I. Noshadi, A.D. Lassaletta, S. Gangadharan, A. Tamayol, A. Khademhosseini, N. Annabi, A highly adhesive and naturally derived sealant, Biomaterials 140 (2017) 115–127.
[42] K. Yue, G. Trujillo-de Santiago, M.M. Alvarez, A. Tamayol, N. Annabi, A. Khademhosseini, Synthesis, properties, and biomedical applications of gelatin methacryloyl (GelMA) hydrogels, Biomaterials 73 (2015) 254–271.
[43] A. Narayanan, Y. Xu, A. Dhinojwala, A. Joy, Advances in photoreactive tissue adhesives derived from natural polymers, ChemEngineering 4 (2) (2020) 32.
[44] M. Araki, H. Tao, N. Nakajima, H. Sugai, T. Sato, S.H. Hyon, T. Nagayasu, T. Nakamura, Development of new biodegradable hydrogel glue for preventing alveolar air leakage, J. Thorac. Cardiovasc. Surg. 134 (5) (2007) 1241–1248.
[45] M. Takaoka, T. Nakamura, H. Sugai, A.J. Bentley, N. Nakajima, N.J. Fullwood, N. Yokoi, S.H. Hyon, S. Kinoshita, Sutureless amniotic membrane transplantation for ocular surface reconstruction with a chemically defined bioadhesive, Biomaterials 29 (19) (2008) 2923–2931.
[46] Z. Jian, T. Zhuang, T. Qinyu, P. Liqing, L. Kun, L. Xujiang, W. Diaodiao, Y. Zhen, J. Shuangpeng, S. Xiang, H. Jingxiang, L. Shuyun, H. Libo, T. Peifu, Y. Qi, G. Quanyi, 3D bioprinting of a biomimetic meniscal scaffold for application in tissue engineering, Bioact Mater 6 (6) (2021) 1711–1726.
[47] R. Leu Alexa, H. Iovu, J. Ghitman, A. Serafim, C. Stavarache, M.M. Marin, R. Ianchis, 3D-Printed gelatin methacryloyl-based scaffolds with potential application in tissue engineering, Polymers 13 (5) (2021).
[48] M. Takaoka, T. Nakamura, H. Sugai, A.J. Bentley, N. Nakajima, N. Yokoi, N. J. Fullwood, S.H. Hyon, S. Kinoshita, Novel sutureless keratoplasty with a chemically defined bioadhesive, Invest. Ophthalmol. Vis. Sci. 50 (6) (2009) 2679–2685.
[49] P. Pedram, C. Mazio, G. Imparato, P.A. Netti, A. Salerno, Bioinspired design of novel microscaffolds for fibroblast guidance toward in vitro tissue building, ACS Appl. Mater. Interfaces 13 (8) (2021) 9589–9603.
[50] S.M. Lien, L.Y. Ko, T.J. Huang, Effect of pore size on ECM secretion and cell growth in gelatin scaffold for articular cartilage tissue engineering, Acta Biomater. 5 (2) (2009) 670–679.
[51] N. Annabi, J.W. Nichol, X. Zhong, C. Ji, S. Koshy, A. Khademhosseini, F. Dehghani, Controlling the porosity and microarchitecture of hydrogels for tissue engineering, Tissue Eng. B Rev. 16 (4) (2010) 371–383.
[52] M.W. Grinstaff, Designing hydrogel adhesives for corneal wound repair, Biomaterials 28 (35) (2007) 5205–5214.
[53] T.J. van den Berg, K.E. Tan, Light transmittance of the human cornea from 320 to 700 nm for different ages, Vis. Res. 34 (11) (1994) 1453–1456.
[54] B. Duchesne, H. Tahi, A. Galand, Use of human fibrin glue and amniotic membrane transplant in corneal perforation, Cornea 20 (2) (2001) 230–232.
[55] J.I. Ahn, L. Kuffova, K. Merrett, D. Mitra, J.V. Forrester, F. Li, M. Griffith, Crosslinked collagen hydrogels as corneal implants: effects of sterically bulky vs. non-bulky carbodiimides as crosslinkers, Acta Biomater. 9 (8) (2013) 7796–7805.
[56] F. Stoeckel, J. Konnerth, W. Gindl-Altmutter, Mechanical properties of adhesives for bonding wood—a review, Int. J. Adhesion Adhes. 45 (2013) 32–41.
[57] L. Zhou, C. Dai, L. Fan, Y. Jiang, C. Liu, Z. Zhou, P. Guan, Y. Tian, J. Xing, X. Li, Injectable self-healing natural biopolymer-based hydrogel adhesive with thermoresponsive reversible adhesion for minimally invasive surgery, Adv. Funct. Mater. 31 (14) (2021), 2007457.
[58] S.E. Wilson, Corneal myofibroblasts and fibrosis, Exp. Eye Res. 201 (2020) 108272.
[59] W.J. Reinhart, D.C. Musch, D.S. Jacobs, W.B. Lee, S.C. Kaufman, R.M. Shtein, Deep anterior lamellar keratoplasty as an alternative to penetrating keratoplasty a report by the american academy of ophthalmology, Ophthalmology 118 (1) (2011) 209–218.
[60] J. Myerscough, C. Bovone, P.B.M. Thomas, M. Mimouni, F. Aljassar, S. Padroni, M. Busin, Sutureless superficial anterior lamellar keratoplasty for recurrent corneal haze after repeat excimer laser surface ablation, Br. J. Ophthalmol. 104 (3) (2020) 341–344.
[61] Z. Wu, Y. Zhou, N. Li, M. Huang, H. Duan, J. Ge, P. Xiang, Z. Wang, The use of phospholipase A(2) to prepare acellular porcine corneal stroma as a tissue engineering scaffold, Biomaterials 30 (21) (2009) 3513–3522.
[62] Y.H. Huang, F.W. Tseng, W.H. Chang, I.C. Peng, D.J. Hsieh, S.W. Wu, M.L. Yeh, Preparation of acellular scaffold for corneal tissue engineering by supercritical carbon dioxide extraction technology, Acta Biomater. 58 (2017) 238–243.
[63] S.Y. Cho, M.S. Kim, S.J. Oh, S.K. Chung, Comparison of synthetic glues and 10-0 nylon in rabbit lamellar keratoplasty, Cornea 32 (9) (2013) 1265–1268.
[64] A. Abdelkader, S.M. Elewah el, H.E. Kaufman, Confocal microscopy of corneal wound healing after deep lamellar keratoplasty in rabbits, Arch. Ophthalmol. 128 (1) (2010) 75–80.
[65] N.A. Frost, J. Wu, T.F. Lai, D.J. Coster, A review of randomized controlled trials of penetrating keratoplasty techniques, Ophthalmology 113 (6) (2006) 942–949.
[66] K. Pang, L. Du, K. Zhang, C. Dai, C. Ju, J. Zhu, X. Wu, Three-dimensional construction of a rabbit anterior corneal replacement for lamellar keratoplasty, PloS One 11 (12) (2016), e0168084.